CHALMERS
UNIVERSITY OF TECHNOLOGY

Scenario-based Stochastic Optimization for Energy and Flexibility Dispatch of a Microgrid

Scenario-based Stochastic Optimization for Energy and Flexibility Dispatch of a Microgrid

Kyriaki Antoniadou-Plytaria, *Graduate Student Member, IEEE*, David Steen, Le Anh Tuan, *Member, IEEE*, Ola Carlson, Baraa Mohandes, *Member, IEEE*, and Mohammad Ali Fotouhi Ghazvini

***Abstract*—Energy storage is one of the most important components of microgrids with non-dispatchable generators and can offer both energy and flexibility services when the microgrid operates in grid-connected mode. This paper proposes a scenario-based stochastic optimization model that can be used to determine the energy and flexibility dispatch of a residential microgrid with solar and stationary battery systems. The objective of the model is to minimize the expected energy and peak power cost as well as the battery aging cost, while maximizing the expected revenue from flexibility. The formulated stochastic optimization problem is solved in rolling horizon with the uncertainty model being dynamically updated to consider the most recent forecast profiles for solar power and electricity demand. The benefits of the proposed approach were demonstrated by simulating the daily operation of a real building. The results showed that the estimated flexibility was successfully dispatched yielding an economic value of at least 7% of the operation cost of the building microgrid. The model can be used by flexibility providers to assess their flexibility and design a bidding strategy as well as by system operators to design incentives for flexibility providers.**

***Index Terms*—Battery degradation, battery energy storage, flexibility, microgrids, renewable energy, stochastic optimization.**

NOMENCLATURE

Sets

$\mathcal{H}$	Set of time steps (simulation horizon).
$\mathcal{H}_f$/$\mathcal{H}_{f'}$	Set of time steps belonging to the flexibility activation period.
$\mathcal{I}$/$\mathcal{K}$	Set of discharging/charging sample data.
$\mathcal{W}$	Set of scenarios.

Indices

i/k	Index for discharging/charging sample data.
t	Index for time (discretization) steps.
w	Index for scenarios.

Parameters

$P^L_{t,w}$	Active load.
$P^{PV}_{t,w}$	Active power from solar generation.
SoE_{max}	Upper state-of-energy limit of the battery.
SoE_{min}	Lower state-of-energy limit of the battery.
H	Percentage of end-of-life retained battery capacity.
Λ_t	Spot price [$/kWh].
C_i	Grid charge for energy transmission [$/kWh].
Π_w	Probability of occurrence.
C_e	Reimbursement fee paid to producers of small-scale generation [$/kWh].
Δt	Length of time discretization step (time interval).
E_{max}	Installed battery capacity [kWh].
$C^{B,0}$	Purchase cost of battery [$].
C_{pp}	Power-based grid tariff [$/MW/month].
$\mathcal{E}^{PV}_t$/$\mathcal{E}^L_t$	Forecast error of PV generation/load demand.
σ^{PV}_t/σ^L_t	Standard deviation of probability distribution of the forecast error of PV generation/load demand.
η^{ch}_t/η^{dis}_t	Charging/discharging efficiency of the battery.
P^-_i/P^+_i	Sample measurements of output/input power from/to the battery cells.
P^{dis}_i/P^{ch}_i	Sample measurements of discharging/charging power to/from the grid.
SoE^{dis}_i	Sample measurements of battery energy storage state-of-energy during discharging.
SoE^{ch}_k	Sample measurements of battery energy storage state-of-energy during charging.
B_1,B_2	Cycle aging coefficients.
C_{flex}	Flexibility price [$/kW].
C_{pen}	Penalty [$/kW] for not providing the flexibility.
I_c	Average charging C-rate.
P^L_{peak}	Upper capacity limit.

Variables

c^{im}	Expected cost of imported energy [$].
c^p	Expected cost of peak imported power [$].
f/f'/f''	Value of the microgrid's objective function.
f^{flex}	Value of the microgrid's objective function when there is a flexibility request.
$p^{im}_{t,w}$/$p^{ex}_{t,w}$	Imported/exported power from/to the grid.
r^{ex}	Expected revenue of exported energy [$].
r^{flex}	Expected revenue from offering flexibility [$].
p^-_t/p^+_t	Output/input power from/to the battery cells.
p^{dis}_t/p^{ch}_t	Discharging/charging power to/from the grid.
q	Battery capacity loss in %.
soe_t	State-of-energy of the battery energy storage.
x_{ti}/y_{tk}	Positive variables indicating choice of discharging/charging samples i/k.
$\beta_{t,w}$	Deviation from flexibility bid.
$p^{fl,p}$	Expected peak imported power during the flexibility activation period.
p^{flex}	Amount of active power flexibility.
$p^{Max,net}_w$	Peak net power exchange of scenario w during the flexibility activation period.
c^B	Cost of cycle-based battery degradation in [$].

This work has received funding from the European Union's Horizon 2020 research and innovation programme under grant agreement No 864048.

Kyriaki Antoniadou-Plytaria, David Steen, Le Anh Tuan, and Mohammad Ali Fotouhi Ghazvini are with the Department of Electrical Engineering, Chalmers University of Technology, Hörsalsvägen 11, SE-412 96 Göteborg, Sweden. Baraa Mohandes is with Luxembourg Institute of Science in Technology (LIST), 5, Avenue des Hauts-Fourneaux, L-4362, Esch-sur-Alzette, Luxembourg.

I. Introduction

THE increase in the integration of renewable-based generation also increases the flexibility needs of system operators [1]. To avoid the operation of expensive and fossil-fuel based generators for the sole purpose of containing infrequent high-peak periods, new flexibility sources are urgently needed. These will also offer significant cost savings [2]. Such flexible sources can include distributed energy resources (DERs) and demand response resources at distribution system level, which can offer demand-side flexibility services (FSs).

The distribution system operator (DSO) can act as the intermediate responsible party for technical validation of demand-side FSs traded in day-ahead and intra-day markets or s/he can act as the flexibility procurer [3]. Local FSs can offer both economic and sustainable solutions for the future challenges and unplanned issues concerning the distribution grid operation. Although DSOs deem FSs less reliable compared to network reinforcement/expansion, flexibility is a solution that can be available more quickly than any network upgrade, which can take up to 10-12 years. Moreover, demand-side FSs can mitigate the impact of the high-peak conditions incurring lower capital expenditures compared to the upgrade of distribution grid infrastructure or even to other FSs such as grid reconfiguration [4]. Even if the network reinforcement costs cannot altogether be avoided, deferring these costs with the support of FSs can be economically beneficial.

Flexibility offered by stationary battery energy storages (BESs), in particular, is gaining ground, since it can mitigate imbalances between load and supply close to real-time thanks to the short ramp-up and ramp-down time. Moreover, if these BESs are coupled together with renewable-based generation at the distribution level, they can lead to the formation of clusters that resemble grid-connected microgrids (MGs). These MGs can be formed by a number of geographically contiguous assets and consumers such as the residents of a building or a neighborhood of buildings. These consumers that benefit from the energy services (ESs) and/or FSs provided by the MG are called MG customers. The ability of the MGs to integrate smart, innovative technologies and modernize the existing grid can facilitate FSs offered by the MG resources that can benefit both the MG customers and the DSOs.

A. State-of-the-Art

The ideas of flexibility quantification and demand-side FSs provided from DERs or DERs aggregators such as MG operators have recently gained attention, as is evident by a number of studies e.g., [1], [4]–[11]. The real-time quantification of flexibility, which is critical for modeling and implementing any FS, is a research gap addressed by few works only e.g., [5], [6]. Ref. [4] presents a rudimentary model of a FS offered by a large heat pump with predetermined cost of activation and discrete steps of flexibility amounts. The MG flexibility bids are assumed to be equal to the predicted power injected to the main grid in the hour-ahead bidding process of [7], where solar irradiance uncertainty is considered in the BES-based MG energy scheduling using a Markov transition matrix and the recursive least-squares method for predictions; the load uncertainties are disregarded. The use of the BES as a buffer to correct hourly mismatches between injected power and bids might require investments on larger capacity or reduce income from other revenue streams, as less capacity is released to provide services. Unlike aforementioned studies, which use model-based approaches, machine learning techniques are proposed in [8] to forecast the longevity of the offered flexibility. Similarly, a regression model is used in [9] to design the incentives that will increase the participation of residential energy hubs in FSs. However, none of the studies [5], [7]–[9] integrate the FS in the optimal economic dispatch problem (note that in this paper, the terms scheduling and dispatch are used interchangeably).

The impact of FSs in the economic energy scheduling of MGs was considered in [1], [6], [10], [11]. The concept of the flexibility envelopes is used in [6] to consider the feasibility region of the real-time operational flexibility of a MG in its optimal power dispatch, which is solved in receding (rolling) horizon (RH). The power exchange with the main grid is assumed to be known per time step, thus the BES flexibility dispatch satisfies the MG needs to avoid the cost of dispatching diesel generators or curtailing load. A scenario-based stochastic optimization (SO) problem is solved for a grid-connected MG in [10], [11], where the problem integrates flexibility limits. In [10] these limits are time-varying and depend on the net consumption of the rest of customers connected to the same distribution feeder as the MG. In [11], these limits are set by the DSO to minimize deviations from the approved power exchange schedule, which is treated as a baseline power profile. Similarly, the scheduled power exchange is used as a baseline reference to define MG flexibility in [1], where a cooperative controller based on model predictive control is used to distribute the flexibility amount among a network of MGs. However, using the MG schedule as a baseline to define MG flexibility can be prone to manipulation [12] and having to agree on a power exchange schedule can be problematic for a real-world implementation of this FS.

As the above literature review showed, with regard to flexibility, studies mostly focus on estimating the technically available flexibility or take into account its economic impact to the energy dispatch of the DERs. The technically available flexibility refers to the estimated flexibility amounts that are feasible according to the technical operation of the DERs as in [1], [4], [6]–[9], [11]. It can also refer to flexibility which is admissible by the network operation [13] and even further restricted to secure the network's reliability [14] or robustness against uncertainties [15]. It does not, however, consider the "willingness" of the FS provider (FSP) to offer a feasible amount of flexibility i.e., the economically viable or optimal flexibility. Even when studies embed FSs into optimal energy scheduling models, the flexibility potential is not explicitly calculated, leading to a lack of quantification and evaluation of the flexibility, especially at distribution level [16]. The flexibility amount that is dispatched solely depends on the operational limits and the grid operator set-points, which are

usually arbitrarily chosen power exchange references. Thus, these works do not give insight regarding the economic value of intra-day flexibility in the presence of uncertainties for either the FSP or the procurer of flexibility.

B. Paper Contributions and Structure

The advancement beyond state of the art brought by this paper is the quantification of the MG flexibility using a probabilistic approach. While the previously developed flexibility quantification methodologies only evaluated the technically available flexibility, this paper introduces a methodology that quantifies the flexibility amounts that are both feasible and economically optimal in different uncertainty realizations under a scenario-based SO model. Flexibility is explicitly computed considering: 1) uncertainties (in both power supply and demand), 2) the market-based energy scheduling strategy of the MG, and 3) the model of a capacity limitation FS [17], which does not depend on baseline reference profiles. Moreover, thanks to the closed-loop (CL) control approach applied for the MG energy scheduling, the effect of the forecast error is minimized and the dispatch of the desired flexibility is achieved to the extent that it is feasible.

Based on these, the paper made the following contributions:

- A SO model solved in RH scheme for the optimal market-based energy scheduling of a MG taking into account BES degradation and uncertainty related to the load demand and photovoltaic (PV) power output. Unlike the RH approach in [18], which also considers BES degradation and uncertainties in the optimal BES scheduling solved by stochastic dynamic programming, each update in the forecast updates the whole BES control trajectory, while the BES power is not discretized and thus the impact of the forecast error is even further minimized.
- The integration of a local FS model in the energy scheduling model. The resulting energy and flexibility dispatch SO problem is used when there is a flexibility request by the DSO to calculate the optimal flexibility bid (offer) and the expected revenue from offering this FS.
- A methodology for stochastic assessment and dispatch of technically and economically available flexibility. This methodology can be used to dispatch intra-day flexibility on a short notice (up to close to real-time) to alleviate unscheduled network congestions (i.e., unrelated to network maintenance). It can also be used to define flexibility evaluation metrics and can easily be adjusted to fit the specific needs of the flexibility procurer.
- A case study that demonstrates the effect of BES capacity and flexibility price on the dispatched flexibility and daily economic value of flexibility for the MG customers.

It should be noted that the proposed methodology is useful to both the flexibility procurers i.e., grid operators, and the FSPs. The FSPs can take informed decisions regarding their participation in FSs and they can use this methodology to appropriately design their bidding strategy in flexibility markets. The grid operators can assess end-user flexibility and estimate its value in improving the network operation. Considering the increased uncertainties introduced at the distribution level, it is necessary to study the impact of a wide range of flexibility prices in order to appropriately design incentive mechanisms that ensure the dispatch of the flexibility as specified by the needs of the system operation.

The rest of the paper is organized as follows. Section II presents the mathematical formulation of the MG's energy scheduling optimization model. Section III explains the uncertainty modeling, while Section IV elaborates on the process of flexibility evaluation and dispatch. Simulation results are given in Section V and conclusions are drawn in Section VI.

II. Stochastic Energy and Flexibility Dispatch

This section presents the formulation of the SO model that is used to solve the energy and flexibility dispatch problem for a building MG with PV systems and a stationary BES, which is used as a flexible resource. This problem is solved by the MG energy management system (MG-EMS), which integrates the SO model. The solution yields a set of BES power dispatch set-points that maximize the economic benefits of the MG customers, whose electricity demand is satisfied from the MG resources and the upstream grid connection.

The MG operator has a contract with an electricity retail provider, which enables energy trading at wholesale electricity market price. At the same time, the MG operator has a contract for flexibility provision with a DSO, which purchases and utilizes this flexibility. The contract for ESs enables the MG operator to reduce the energy costs performing load shifting and energy price arbitrage. The contract for FSs allows the DSO to request and buy a FS from the MG on a short notice within a day to solve unexpected operation problems or improve operation, utilizing the most recent information (e.g., forecasts). In addition, the DSO can buy this FS to satisfy balancing needs of the transmission, although it should be noted that the FS considered in this paper is only used by the DSOs. If there are requirements on minimum flexibility amounts that the MG does not meet, the FS can be offered through an aggregator.

A. Scenario-based SO Model

The objective of this model is to minimize the MG's operation cost for the next look-ahead period considering uncertainties in electricity load demand and PV generation. Forecasts of PV generation and load, as well as information about the statistical distribution of forecast errors, are used as input to the integrated SO model. The time horizon length is appropriately chosen to avoid the need of forecasting the electricity prices. The MG cost includes the energy cost (which can take a negative value, as the income from selling energy is being subtracted), the cost due to peak power charge, the BES degradation cost, and the income from offering flexibility.

1) Objective Function: As explained above, the objective function is to minimize the expected (over the dispatch period) cost f^{flex} of a MG that can offer a FS and is given by:

$$\min f^{flex} = c^{im} - r^{ex} + c^{p} + c^{B} - r^{flex}, \qquad (1)$$

where

$$c^{im} = \sum_{t\in\mathcal{H}} \sum_{w\in\mathcal{W}} \Pi_w(\Lambda_t + C_i) p^{im}_{t,w} \Delta t, \tag{2}$$

$$r^{ex} = \sum_{t\in\mathcal{H}} \sum_{w\in\mathcal{W}} \Pi_w(\Lambda_t + C_e) p^{ex}_{t,w} \Delta t, \tag{3}$$

$$r^{flex} = C_{flex} p^{flex} = C_{flex}(P^L_{peak} - p^{fl,p}). \tag{4}$$

In (1), the first term (c^{im}) is the expected cost of the imported energy and the second term (r^{ex}) is the expected revenue associated with the energy exported to the grid. The term c^B denotes the cost of BES degradation (expressed as capacity loss) due to cycle aging, c^p is the expected cost for the peak power drawn from the main grid, and r^{flex} is the expected reward for providing flexibility. Eq. (2)–(4) analytically present the values of c^{im}, r^{ex}, and r^{flex}. The scheduling horizon and the length of time intervals are shown by $\mathcal{H}$ and Δt, respectively. The positive variables $p^{im}_{t,w}/p^{ex}_{t,w}$ are the imported/exported power from/to the grid at time step t and scenario w, while Π_w is the probability of occurrence of scenario w. The electricity wholesale market is denoted by Λ_t, while C_i is the grid charge for energy transmission (grid utilization), and C_e is the reimbursement fee paid by the DSO as an incentive to reduce network losses. To calculate the value of c^p the following constraint is added

$$c^p \geq C_{pp} \sum_{w\in\mathcal{W}} \Pi_w p^{im}_{t,w}, \ \forall t \in \mathcal{H}, \tag{5}$$

where the power tariff C_{pp} is linked to the maximum average power of the studied period (measured per time step Δt). The positive variable p^{flex} denotes the amount of active power flexibility (average value over Δt), which is also the flexibility bid, C_{flex} is the flexibility price, and $p^{fl,p}$ is the expected peak imported power during the flexibility activation period. Note that the amount of flexibility is calculated in terms of power capacity reduction. When flexibility is activated, the MG resources modify their schedule to guarantee that the peak imported power will not exceed the "new" capacity $P^L_{peak} - p^{flex}$ provided by the FS. The parameter P^L_{peak} should be based on a value that the DSO and the MG operator can easily agree upon such as e.g., the capacity at the grid connection point, so that the flexibility can be quantified in a reliable manner. Fig. 1 depicts p^{flex} and, in addition, it shows an illustrative diagram of the MG resources and the power flows among the resources and the upstream connected AC grid.

2) Power Balance: As can be seen in Fig. 1, the converter that couples together the BES and the PV systems has bi-directional operation. Therefore, both the PV power and the BES discharging power can supply the building demand and be exported to the AC grid. Moreover, the BES can be charged through both the upstream AC grid and the PV systems. Thus, the power balance of the MG is given by

$$P^{PV}_{t,w} + p^{dis}_t - p^{ch}_t = p^{ex}_{t,w} - p^{im}_{t,w} + P^L_{t,w}, \forall t \in \mathcal{H}, \forall w \in \mathcal{W}, \tag{6}$$

where $P^{PV}_{t,w}$, $P^L_{t,w}$, and the positive variables p^{ch}_t/p^{dis}_t respectively refer to PV generation, electric power consumption of the building, and charging/discharging power of the BES. The losses of the grid side converter are ignored.

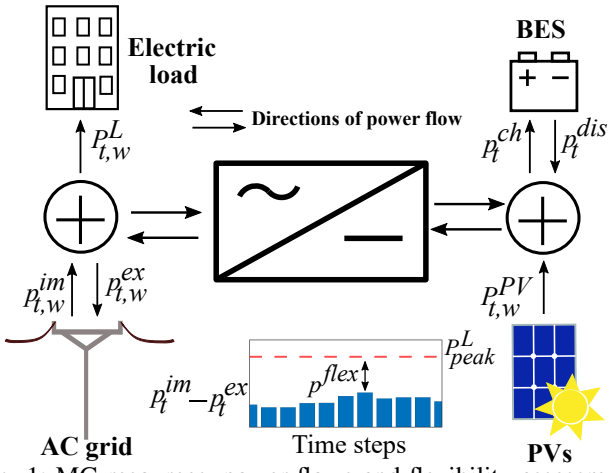

Fig. 1: MG resources, power flows and flexibility assessment.

3) BES Model: The BES model is given by (7)–(17). This is a measurement-based model, which was first presented in [19] and later expanded in [20] in order to include the BES degradation model presented in [21] and modified in [22] and [23] to express the BES capacity loss as a function of cumulative energy throughput. The model uses a sampling-based approach on data from charging/discharging curves in order to capture the behavior of an actual BES more accurately compared to typical linear BES models used in optimization models. The parameters $SoE^{ch}_k, P^+_k, P^{ch}_k, SoE^{dis}_i, P^-_i, P^{dis}_i$ take the values of the sample data. The positive variables p^-_t/p^+_t represent power output/input from/to the BES cells respectively, before/after BES losses have been taken into account. Moreover, E^{max} is the installed BES capacity and soe_t is the state-of-energy (SoE), constrained by the lower/upper limits denoted by SoE^{min}/SoE^{max} (these limits are typically suggested by manufacturers to increase the BES lifetime [24], [25]). The continuous variables $x_{i,t}$ and $y_{k,t}$, which are associated respectively with the choice of discharging or charging sample data, are used to create convex combinations of soe_t, p^+_t, p^{ch}_t. This model takes into account the variable (with respect to BES power and SoE) charging/discharging efficiencies of the BES system (both internal BES losses and DC/DC converter losses are considered), which are defined as $\eta^{ch}_t = p^+_t/p^{ch}_t$ and $\eta^{dis}_t = p^{dis}_t/p^-_t$, respectively, $\forall t \in \mathcal{H}$ [19].

$$soe_t = soe_{t-1} + \frac{p^+_{t-1}\Delta t}{E_{max}} - \frac{p^-_{t-1}\Delta t}{E_{max}}, \ \forall t \in \mathcal{H} \tag{7}$$

$$SoE_{min} \leq soe_t \leq SoE_{max}, \ \forall t \in \mathcal{H}, \tag{8}$$

$$p^-_t = \sum_{i\in\mathcal{I}} P^-_i x_{ti}, \ \forall t \in \mathcal{H}, \tag{9}$$

$$p^{dis}_t = \sum_{i\in\mathcal{I}} P^{dis}_i x_{ti}, \ \forall t \in \mathcal{H}, \tag{10}$$

$$p^+_t = \sum_{k\in\mathcal{K}} P^+_k y_{tk}, \ \forall t \in \mathcal{H}, \tag{11}$$

$$p^{ch}_t = \sum_{k\in\mathcal{K}} P^{ch}_k y_{tk}, \ \forall t \in \mathcal{H}, \tag{12}$$

$$soe_t = \sum_{i\in\mathcal{I}} SoE_i^{dis} x_{ti} + \sum_{k\in\mathcal{K}} SoE_k^{ch} y_{tk},\ \forall t \in \mathcal{H}, \tag{13}$$

$$\sum_{i}^{I} x_{i,t} = 1,\ 0 \le x_{i,t} \le 1,\ \forall t \in \mathcal{H}, \tag{14}$$

$$\sum_{k}^{K} y_{k,t} = 1,\ 0 \le y_{k,t} \le 1,\ \forall t \in \mathcal{H}. \tag{15}$$

The BES capacity loss (%) due to cycle aging is given by:

$$q = B_1 e^{B_2 I_c} \sum_{t\in\mathcal{H}} (p_t^- + p_t^+)\Delta t. \tag{16}$$

The parameters B_1 and B_2 were obtained from empirical fitting of experimental data, while the parameter I_c is the daily average C-rate. The BES cost used in (1) is calculated as:

$$c^B = \frac{C^{B,0} q}{100\% - H}, \tag{17}$$

where q is multiplied with the installation cost $C^{B,0}$ and divided by the maximum acceptable capacity loss $(100\% - H)$ before the BES is retired (H is the end-of-life retained capacity percentage in %). Thus, if $q = 100\% - H$ then $c^B = C^{B,0}$, since the BES must be replaced.

4) FS Model: The type of FS considered in this study is a capacity limitation service as introduced in [12]. Constraints (18)–(19) are added to model this FS:

$$p^{fl,p} \ge \sum_{w\in\mathcal{W}} \Pi_w p_w^{Max,im}, \tag{18}$$

$$p_w^{Max,net} \ge (p_{t,w}^{im} - p_{t,w}^{ex}),\ \forall w \in \mathcal{W}, \forall t \in \mathcal{H}_f, \tag{19}$$

where the variable $p_w^{Max,net}$ is the net power peak of scenario w during the flexibility activation period $\mathcal{H}_f \subseteq \mathcal{H}$. With this FS, when the FSP (in this case the MG operator) activates the flexibility, the dispatch of the BES power seeks to satisfy the flexibility bid p^{flex}, which will be achieved if the MG net power peak during the flexibility activation period does not exceed the value of variable $p^{fl,p}$.

B. RH Approach

The model presented in Section II-A can be used to solve the SO problem either in open-loop (OL) or in CL i.e., in RH, as can be seen in Fig. 2. In OL control, the problem is solved once to determine the BES operation set-points which will be applied in the next time period. In CL control, only the next time-step optimal set-points are implemented. Then, the scheduling horizon is shifted and the same problem (that was solved only once in the OL control) is solved again. This is repeated multiple times (depending on the choice of time discretization step) to obtain the BES set-points of the same time period as in OL. After the time horizon is shifted and before the next simulation, the forecast profiles are updated to consider the most recently available forecasts and include the part of the time horizon that was not considered in the previous simulation. Note here that the term RH often appears under the name "model predictive control" in literature [26],

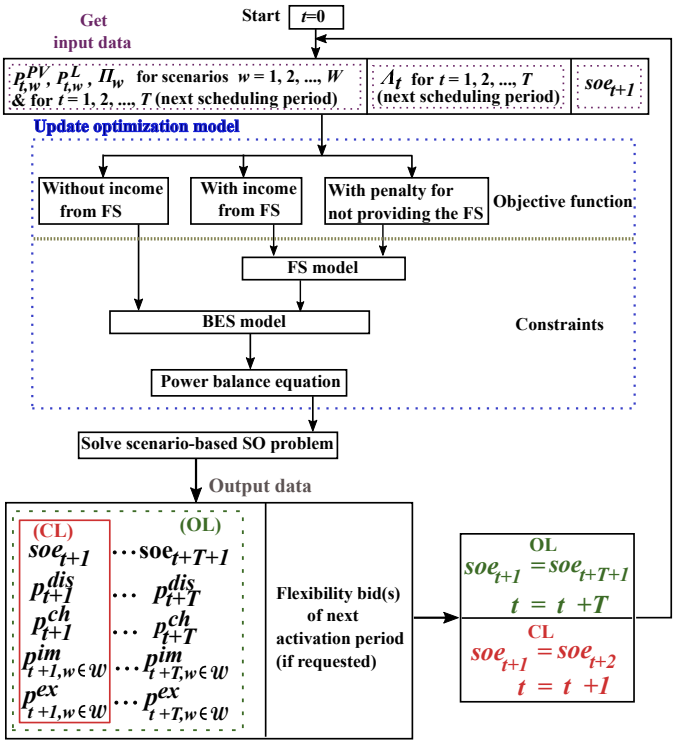

Fig. 2: Flowchart of the MG energy and flexibility dispatch.

typically when the problem is formulated using state-space representation instead of mathematical programming, which was used for the formulation of the SO model of this paper.

Most studies apply SO in OL. Even though the RH approach reduces the effect of the forecast errors by dynamically updating the set-points, it requires more frequent simulations, which can be an issue as SO has higher computation time than deterministic optimization. Similar to [27], both the SO and the RH approach will be used in this paper to benefit from the feedback, which is particularly important for close to real-time control. In order to reduce the size of the SO problem and avoid scalability issues, deterministic control variables were used in the model in Section II-A i.e., the scheduled BES power is independent of the scenario. Since the RH approach is used, it is only the next time-step control decisions that are implemented after each simulation and the deterministic control trajectory can be updated considering the latest forecasts available with every new simulation. The rest of the control trajectory of each simulation is advisory. The MG power import and export, which are dependent on the BES power (deterministic variable) and the electricity demand and PV generation (stochastic input parameters), are the stochastic decision variables of the optimization problem. Despite the advantages of the RH approach, the OL control can be useful for practical applications in case of failure to receive feedback. Then, the advisory BES power set-points obtained from the last solution of the SO problem will be applied, thus implementing OL control until the CL control can be restored.

III. Uncertainty Modeling

The main uncertainty modeling approaches include [28]: 1) *scenario-based SO and RO*, where it is assumed that uncertainty is adequately characterized by a set of future event scenarios each of them associated with the probability of occurrence of the event, 2) *adaptive RO and chance-constrained optimization (CCO)*, which use uncertainty sets to constrain the operating points, 3) *Markov decision processes (MDPs)*, where the uncertainty is only modeled for the next-step decision, and 4) *reinforcement learning (RL)*, which observes (instead of explicitly modeling) uncertainty.

A. Comparative Discussion of Modeling Approaches

All the previously mentioned approaches have been used in MG energy management studies. Depending on the application they can offer advantages regarding computation time, feasibility, and solution cost.

1) Optimization Approaches: The main drawbacks of RO and CCO are the too conservative (and by extent costly) solutions of the former and the arbitrarily chosen constraint violation levels of the latter. On the other hand, one major benefit of RO and CCO against SO is that they can yield simplified equivalent reformulations of the original optimization problem and reduce its complexity. However, the proposed SO model already considerably reduces the size of the problem. This is achieved by eliminating the "wait and see" decision variables which are used in classical SO; the future scheduling plan consists of deterministic control variables and the only stochastic variables are the imported and exported MG power which are affected by the deterministic control variables and the stochastic inputs (load, PV generation). In other words, the model considers lookahead uncertainty thanks to the stochastic formulation and, instead of considering real-time uncertainty realization, control adjustments are dynamically being implemented with the RH approach to deal with close to real-time uncertainty. In addition, the scenario generation and reduction technique (see Section III-B) further improves the performance of the model by reducing its size. Therefore, it was computationally efficient to perform SO in RH with the proposed model. Since the performance of RO and CCO is heavily dependent on the underlying characteristics of the probability distribution function [29], [30], their computational advantage would be trivial in this case.

Apart from faster execution, thanks to its deterministic control the proposed SO model also offers certainty of feasible solutions in out-of-sample analysis assuming that the system is properly dimensioned to avoid exceeding the capacity at the point of common coupling with the main grid. Therefore, the other advantage of CCO against classical scenario-based SO, which is the guaranteed satisfaction of the problem's constraints for a specific percentage of the scenarios [31] in an out-of-sample analysis, is not relevant for the proposed model.

2) MDPs: In this case, the problem is formulated in state-space representation and the system state as well as the control output need to be discretized. This leads to the problem well-known as "curse of dimensionality" i.e., to improve the quality of the control more discrete points must be considered which crucially expands the size and the computation time. Formulating the MG energys scheduling as an MDP also enables to solve the problem in RH, as was done in [18], by changing the control strategy or trajectory at each time step depending on the latest forecast information. However, these strategies are pre-determined, whereas solving the SO problem in RH results in a new optimal strategy at each time step.

3) RL: Built on MDP, the optimal strategies are defined without full knowledge of the uncertainty model [32] (or even the MG system). They are rather defined through observation and, therefore, a lot of information is needed as an input to train the RL models, so that they can choose the best "action" i.e., next-step control decision, "on the go". Similar to MDP, the control actions are pre-determined unless the RL model is trained online, which is typically time-consuming.

B. Scenario Generation and Reduction

In order to model stochasticity in scenario-based optimization, the probability distribution of forecast errors of the variable input data must be known. Some studies assume that these errors follow Gaussian distributions [11], [33]. Others use scenario generation algorithms to capture stochasticity and correlations among historical data [34]. To represent the uncertainty associated with the input values in this paper, the day-ahead forecast errors of PV generation and power consumption are assumed to follow the Gaussian distributions given as $\mathcal{E}_t^{PV} \sim N(0, 0.1^2)$ and $\mathcal{E}_t^{L} \sim N(0, 0.05^2)$, respectively, where the standard deviations $\sigma_t^{PV} = 0.1$, $\sigma_t^{L} = 0.05$ were adopted from the day-ahead forecast error distributions of [11], [33]. The accuracy of the forecast values progressively deteriorates for the time steps further ahead in time, which is why B. V. Solanki et al. [35] used non-uniform time resolution. In this paper, the horizon is uniform; however, the standard deviations of the distributions gradually increase to account for the reduction of the intra-day accuracy. Thus, for the time steps until the next hour ahead as well as for the time steps after the first hour and until six hours ahead, they are equal to $10\%\sigma_t^{PV}$/$10\%\sigma_t^{L}$ and $50\%\sigma_t^{PV}$/$50\%\sigma_t^{L}$, respectively. A more detailed uncertainty representation is beyond the scope of this paper and can be a part of future research.

Based on the above-mentioned distributions, a number of scenarios are generated using the Monte Carlo (MC) method i.e., random sampling of the input variables (taken from their most recently updated forecasts) with the added noise to represent forecast error. The forecast profiles have the same time resolution as the time horizon of the simulation i.e., the same number of time discretization steps, and are used as the base scenarios. Since the forecasts are not perfect, a Gaussian random number generator is used to generate an error for each time step of the available load/PV forecast profiles. The values of the base scenarios are then adjusted according to the generated errors and the outcome is one future event scenario of electricity load and PV generation. This process is then repeated to generate all scenarios. After the scenario generation, a mix of fast backward/forward methods in the SCENRED tool

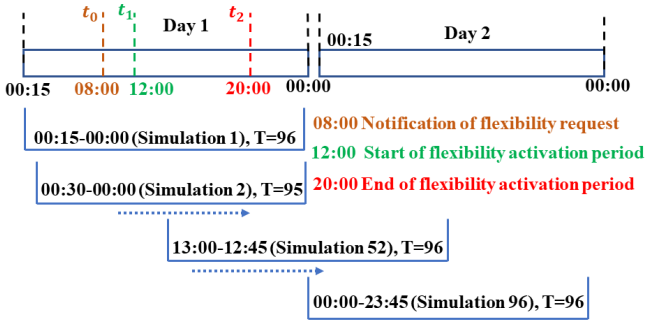

Fig. 3: Process of flexibility dispatch using the RH approach.

of GAMS is used to create a reduced number of scenarios (not equiprobable) which are representative of the real variability of the input values, without substantially compromising the accuracy of the results. A different probability of occurrence is assigned to each scenario by the scenario reduction technique.

IV. Flexibility Assessment and Dispatch

The methodology of flexibility evaluation and dispatch is shown in Fig. 3 with indicative milestones marking the process. This methodology corresponds to an intra-day framework of procuring flexibility. The depicted time discretization step is $\Delta t = 15$ minutes, therefore the energy and flexibility dispatch problem for Day 1 comprises 96 simulations (solutions of the SO problem). As shown in Fig. 3, one simulation is performed at each time step τ to solve the following SO problem

$$\min f = \begin{cases} f' \ (21) & \text{s.t. } (2)\text{–}(17) & \tau < t_0 \\ f^{flex} \ (1) & \text{s.t. } (2)\text{–}(19) & \tau = t_0 \\ f'' \ (22) & \text{s.t. } (2)\text{–}(17),(23),(24) & t_0 < \tau \leq t_2 \\ f' \ (21) & \text{s.t. } (2)\text{–}(17) & t_2 > \tau \end{cases}, \quad (20)$$

$$f' = c^{im} - r^{ex} + c^{p} + c^{B}, \quad (21)$$

$$f'' = c^{im} - r^{ex} + c^{p} + c^{B} - \sum_{t \in \mathcal{H}_{f'}} \sum_{w \in \mathcal{W}} \Pi_w \beta_{t,w} C_{pen}, \quad (22)$$

$$\beta_{t,w} \leq P^{fl,p} - (p^{im}_{t,w} - p^{ex}_{t,w}), \ \forall w \in \mathcal{W}, \ \forall t \in \mathcal{H}_{f'} \quad (23)$$

$$\beta_{t,w} \leq 0, \ \forall w \in \mathcal{W}, \ \forall t \in \mathcal{H}_{f'} \quad (24)$$

where t_0 and t_2 respectively denote the notification time of flexibility request and the end of the flexibility activation period. The MG operator implements the optimal energy schedule obtained from solving the SO problem given by (20) for $\tau < t_0$ at each time step τ. If the DSO needs to buy flexibility, a request is sent at $\tau = t_0$ to the MG-EMS, which responds with the amount p^{flex} and a stochastic assessment of the flexibility that can be offered by solving (20) for $\tau = t_0$. The response is sent directly after the request e.g., in Fig. 3, the flexibility request along with information about the activation period is sent at 08:00 (Simulation 48) and the response is sent to the DSO before the next simulation (at 08:15). The MG-EMS is also notified about the acceptance or decline of p^{flex} before the next simulation. If it is accepted, the MG solves (20) for $t_0 < \tau \leq t_2$ i.e., until the simulation horizon is shifted outside of the activation period (note that $\mathcal{H}_{f'}$ in (22)–(24) refers to the part of the scheduling period that belongs to the flexibility period, which shrinks as the time horizon shifts). In Fig. 3, this problem, which minimizes the mismatch between flexibility bid and dispatch, is solved at each simulation between 08:15-22:00 i.e., Simulations 33-88. Thus, the MG-EMS adjusts its control to provide the flexibility bid both before and during the flexibility activation period which starts at t_1. The mismatch is minimized by penalizing the deviation between the net power and the expected net power peak $p^{fl,p}$, which is now entered as a parameter ($P^{fl,p}$).

The non-negative term $\beta_{t,w}$ in (22)–(24) represents the deviation between the expected peak and dispatched net power that should be penalized at each time step. If the net power is below its expected peak $P^{fl,p}$, which was calculated at t_0 to define the flexibility bid, this deviation should not be penalized. Since the right-side term in (23) becomes positive in this case, (24) becomes the binding constraint and $\beta_{t,w}$ becomes equal to zero because a negative term would increase the value of the cost function f'' given by (22). If the net power exceeds the bid, then (23) is binding and $\beta_{t,w}$ is negative taking the value of $P^{fl,p} - (p^{im}_{t,w} - p^{ex}_{t,w})$. This quantity is multiplied by the penalty C_{pen} adding a cost in f''.

After the look-ahead horizon is shifted past the end of the flexibility activation period, the MG-EMS continues solving the energy scheduling problem given by (20) for $\tau < t_0$. The same problem is also solved after the MG receives a decline of the offered flexibility until there is a new flexibility request. It should be noted that the proposed process of flexibility dispatch is independent of the notification time or the duration of the activation period and can even be used for close to real-time flexibility dispatch, when a small Δt is used. Moreover, the MG response and the notification of acceptance/decline from DSO can occur later than t_0. In that case, the MG-EMS will repeatedly solve (20) for $\tau = t_0$ to optimize the flexibility offer at each time step until it sends the response to the DSO.

Each simulation of the RH process performed at τ can be described by the following steps:

- **Step 1:** The look-ahead horizon extends to include all hours where the electricity price is known, up to a maximum of 24 hours. E.g., in Fig. 3, the initially 24-hour time horizon is continuously reduced by one time step for Simulations 2-51 and then extends again to 24 hours until Simulation 96, since the day-ahead spot market prices are updated at about 12:45 on the previous day [36].
- **Step 2:** Obtain the day-ahead latest updated forecasts of load and PV power output which have the same time resolution as the considered scheduling time horizon. Reduce the length if necessary, update the base scenario, and generate new scenarios.
- **Step 3:** Solve the SO problem according to (20) using the generated scenarios, the price data, and the SoE of the BES that was obtained from the previous simulation. These are the input data illustrated in Fig. 2.
- **Step 4:** Obtain and update set-points p^{dis}_t/p^{ch}_t for $t = 1$. Shift the time horizon by Δt. Go to Step 1 at $\tau + 1$.

V. Simulation Results

The optimal MG energy and flexibility dispatch was simulated for a day considering a grid-connected residential MG as the test system. The optimization models were implemented in GAMS interfaced with CPLEX to solve the linear programming (LP) problems formulated in Section IV. Simulations were performed according to the test cases described in Table I on a PC with 4.2 GHz Intel(R) Core(TM) i7-7700K CPU and 64 GB of RAM.

A. Test System, Input Data, and Parameters

Table II lists the MG characteristics. The electricity load, PV generation, and BES data were obtained from [37], while electricity prices were taken from the Nord Pool market [36] for bidding area 3 of Sweden. The energy and power tariffs (the latter was scaled down to apply to the chosen time horizon) as well as the reimbursement fee were taken from the website of the local DSO [38]. The simulations were repeated for different BES capacities, for comparison and analysis.

The capacity at the connection point was $P^L_{peak} = 43.65$ kW, the time discretization step was $\Delta t = 15$ minutes, and the penalty was $C_{pen} = 180$\$/MW [39]. The values of the BES model parameters in (8) and (16)–(17) were: $B_1 = 0.0013$, $B_2 = 0.3534$, $I_c = 0.3$, $H = 80\%$, $SoE_{min} = 10\%$, $SoE_{max} = 90\%$, and the initial SoE was 50%. The flexibility activation periods were between 07:00-20:00, as was requested from small to medium-sized companies offering flexibility in [40]. A base C_{flex} was calculated according to the following assumption: it was assumed that the revenue from offering 1 kW of p^{flex} would be equal to selling 1 kWh of energy at average spot market price at each hour of the activation period. The simulations were conducted considering different flexibility prices within the range of 50%-150% of this base C_{flex}, which was different for each case (depending on the length of $\mathcal{H}_f$ and the method of flexibility dispatch). For each simulation, 2000 scenarios of PV generation and load were generated using the MC method and the probability distributions and their parameters mentioned in Section III. These were then reduced to 120 scenarios.

B. Case Studies: Stochastic Assessment of Flexibility

The stochastic assessment of flexibility was performed at time step $\tau = t_0$ i.e., right after the notification of the flexibility request. The results are obtained by solving at $\tau = t_0$ the respective SO problem as defined in (20).

1) Cases A & B: The simulations showed that p^{flex} generally increased as the BES size increased, which can be observed in Fig. 4 that presents the stochastic assessment of flexibility for Cases A-B at their base C_{flex} for a 7.2, 14.4, and 18 kWh BES. The actual amount of flexibility that the MG provided to the grid in each of the 120 scenarios is depicted as a histogram plot. The x-axis represents the amount of dispatched flexibility $P^L_{peak} - max(p^{im}_{t,w},\ \forall w \in \mathcal{W})$, where $max(p^{im}_{t,w})$ refers to the activation period $\mathcal{H}_f$. The y-axis reports the probability of achieving a specific amount of flexibility (in one or more of the 120 scenarios). Thus, the percentage reported in the y-axis is the weighted sum of the scenarios where a given flexibility amount occurs, divided by the weighted sum of all 120 scenarios (which has a 100% probability of occurrence). The weights are the probabilities of occurrence of each scenario assigned by the scenario reduction technique (see Section III). The vertical dashed line in each plot of Fig. 4 marks the value of p^{flex} implying that the optimal solution involves scenarios where more flexibility is provided, or where the MG might fall short of meeting its bid.

Under circumstances, the MG with the 7.2 kWh BES could offer slightly more flexibility than the MG with the 14.4 kWh BES (compare Fig. 4 (d) and (e)). In this study, this happened due to the late notification time in Case B. The results are illustrated in Fig. 5 (a) and (b) which present the corresponding schedules of Fig. 4 (d) and (e). In Fig. 5, the power profiles are plotted as bar graphs on the left y-axis (positive values correspond to net power consumption and/or BES charging) and the SoE is given as a line plot on the right y-axis. As can be seen, both BESs stayed idle at their initial SoE until $\tau = t_0$ in preparation for the highest consumption period predicted at $\tau > t_2$ and both were almost at SoE_{min} at the end of the day. Hence, it is evident that the 7.2 kWh BES could not decrease energy and peak power cost as much as the 14.4 kWh BES so the revenue from the FS was more important in reducing the total cost under the considered C_{flex}. The 14.4 kWh BES could benefit more from ESs i.e., energy and peak power cost reduction; therefore, more capacity was used for that purpose at the expense of offering flexibility. In Fig. 5 (b) its injected power resulted in up to 2-3 kW lower MG imported power at time steps 83-90 in comparison to Fig. 5 (a), while offering at the same time flexibility only 400 W less than the amount offered by the 7.2 kWh BES. The 18 kWh BES allocated slightly more capacity than the 14.4 kWh BES for the ESs and the rest was used for the FS resulting in a larger p^{flex}.

Comparing Fig. 4 (d) with (a) and Fig. 4 (f) with (c) it can be seen that p^{flex} could be larger in Case B, even though the notification of flexibility request was much closer to the activation period. An explanation for this is that the uncertainty regarding the flexibility dispatch is lower in Case B, since the activation period is shorter and much closer to $\tau = t_0$; therefore, the input data for $t_1 \leq \tau \leq t_2$ are less affected by forecast errors. Despite that, the probability of dispatching the flexibility according to the bid was actually higher in Case A.

2) Case C: In this case, the flexibility is dispatched per time step and the flexibility bid is indexed by t (p^{flex}_t). The simulations showed that with the increase in C_{flex} the probabilities of dispatching certain flexibility amounts at the same time steps would also increase. However, this was not always straightforward, as increasing the probability at one step could come at the expense of the probability at another step. This can be seen in Fig. 6 which presents the probability of flexibility dispatch for E^{max} =7.2 kW at C_{flex} =\$0.01250/kW and C_{flex} =\$0.01875/kW. Eq. (4) was modified as:

$$r^{flex} = \sum_{t \in \mathcal{H}_f} C_{flex} p^{flex}_t = \sum_{t \in \mathcal{H}_f} C_{flex}(P^L_{peak} - p^{fl,p}_t), \quad (25)$$

TABLE I: Test Cases

	Time of Notification	Flexibility Activation Period	Flexibility Assessment and Dispatch
Case A	08:00	12:00-20:00	Flexibility amount over whole activation period
Case B	18:00	19:00-20:00	Flexibility amount over whole activation period
Case C	08:00	12:00-20:00	Flexibility amount per time step of activation period

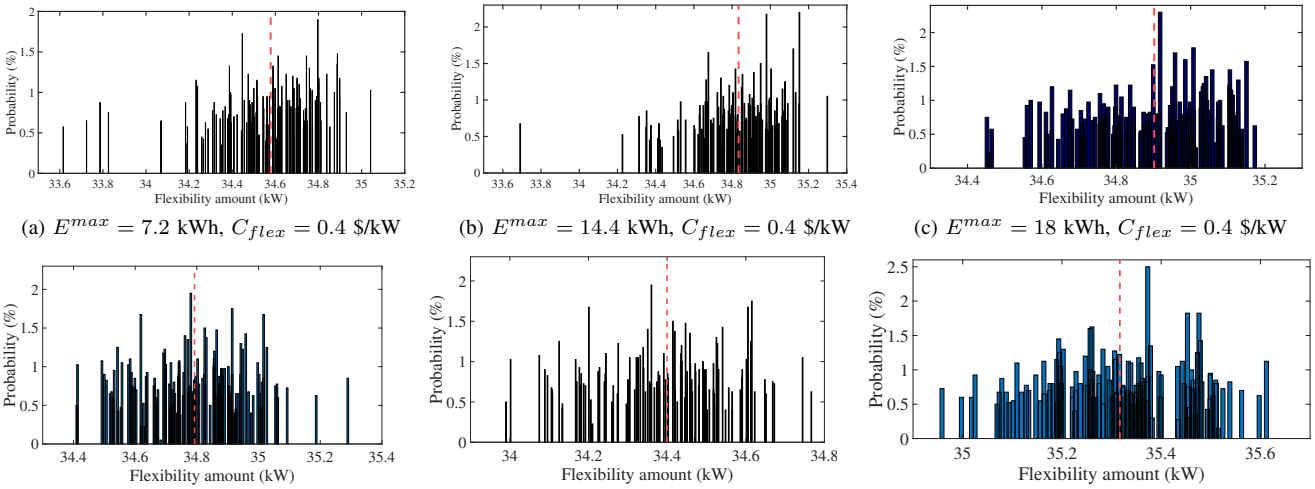

(a) $E^{max} = 7.2$ kWh, $C_{flex} = 0.4$ \$/kW (b) $E^{max} = 14.4$ kWh, $C_{flex} = 0.4$ \$/kW (c) $E^{max} = 18$ kWh, $C_{flex} = 0.4$ \$/kW

(d) $E^{max} = 7.2$ kWh, $C_{flex} = 0.05$ \$/kW (e) $E^{max} = 14.4$ kWh, $C_{flex} = 0.05$ \$/kW (f) $E^{max} = 18$ kWh, $C_{flex} = 0.05$ \$/kW

Fig. 4: The probability distribution of dispatched flexibility and the flexibility bid (dashed line) of the MG operator, considering the base C_{flex} for each case. Fig. (a)-(c) correspond to Case A and Fig. (d)-(f) correspond to Case B.

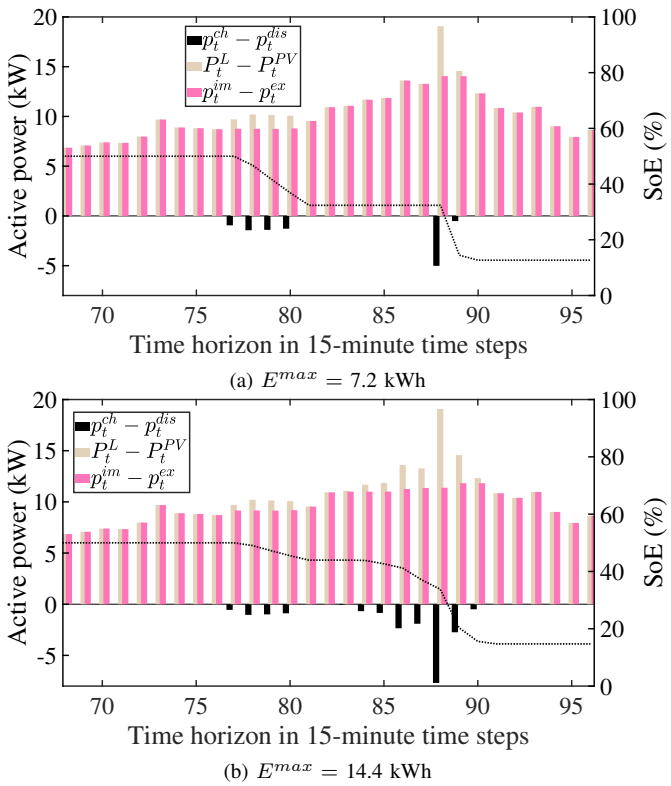

(a) $E^{max} = 7.2$ kWh

(b) $E^{max} = 14.4$ kWh

Fig. 5: MG power flows for Case B with $C_{flex} = 0.05\$/kW$.

TABLE II: Load Demand and DERs of the MG

BES capacity (kWh)	7.2, 14.4, 18
BES energy to power ratio (h)	1.2
Daily electricity consumption (kWh)	162-384
PV capacity (kWp)	13
Peak demand (kW)	32

where $p_t^{fl,p}$, $P_t^{fl,p}$ are also indexed by t and refer to the expected imported power at each time step. The SO problem solved at $\tau = t_0$ is given by the modified objective function f^{flex} s.t. (2)–(17) and (26):

$$p_t^{fl,p} \geq \sum_{w \in \mathcal{W}} \Pi_w (p_{t,w}^{im} - p_{t,w}^{ex}), \ \forall t \in \mathcal{H}_f. \tag{26}$$

The probability of flexibility dispatch in Fig. 6 is shown in the cell numbers of the heatmaps. These correspond to the probability of dispatching a flexibility amount at least equal to the value shown in the *x*-axis, at the time step shown in the *y*-axis. The MG-EMS guaranteed the dispatch of at least 30 kW during the activation period except for time steps 55-58 and at least 35 kW from time step 66 onward for both prices presented in Fig. 6. As can be seen in Fig. 6, the probability of dispatching 30 kW at time step 56 and 35 kW at time steps 63–64 increases with the increase in the price. At the same time, though, the respective probabilities decrease for the amount of 30 kW at time steps 55, 57–58 and the amount of 35 kW at time step 65.

C. Economic Value of Flexibility Dispatch

The probability of dispatching the flexibility amount(s) calculated at $\tau = t_0$ can substantially increase when the SO

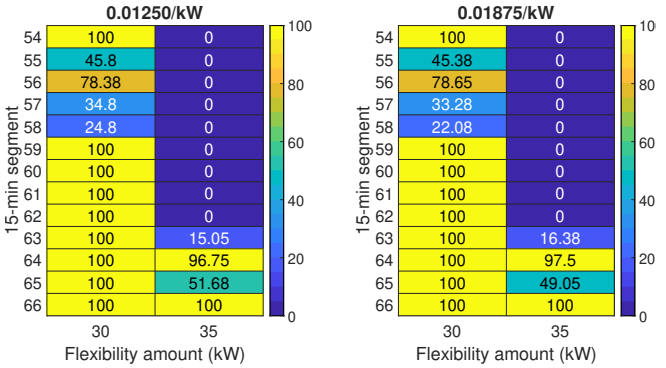

Fig. 6: The probability distribution of dispatched flexibility per time step (Case C, E^{max} =7.2 kW) for two different prices.

problem is solved in RH, depending on the chosen penalty and the technical constraints of the MG resources.

1) Benefit of Solving SO in RH: For all considered values of C_{flex} and E^{max} in Cases A-C, the flexibility amount (p^{flex}) was successfully dispatched. This demonstrated the value of combining SO with the RH approach, which contributed to avoiding the payment of penalties and increased the value of flexibility for the MG operator. The value of flexibility, which was calculated as the cost difference of the daily MG schedule with and without the FS assuming that the base scenario was realized, is shown in Fig. 7 along with the degradation cost and the flexibility bid w.r.t C_{flex}. The value of flexibility was also estimated for the DSO assuming that s/he buys the MG flexibility to reduce the subscription fee that guarantees a certain power level. To calculate this value the cost of buying flexibility was subtracted from the cost reduction achieved by reducing the MG peak imported power using the FS.

2) Factors Affecting the Value of Flexibility: Two important factors associated with the value of flexibility are scrutinized: the BES size and the flexibility dispatch parameters t_0, t_1, t_2 i.e., the time of notification and the duration of the activation period. The results indicated that the proposed FS can offer value to both the MG customers and the DSO when flexibility is dispatched over the whole activation period i.e., in Cases A-B, with the MG's value of flexibility amounting to at least 56% and 7% of the daily MG operation cost, respectively. As can be seen in Fig. 7 (a), (d), and (g), the MG's value of flexibility increased linearly wrt C_{flex}, while the BES size did not significantly affect the MG's daily value of flexibility. This shows that the MG-EMS favored participation in ESs (energy arbitrage, peak shaving) instead of the FS within the studied range of C_{flex}. The BES size played a more important role in the DSO's value. In fact, in Cases A-B, the larger BESs usually increased the economic benefits for the DSO. Case C offered no benefit to the DSO even though the value of flexibility was considerably higher for the MG.

Analyzing the results in Fig. 7 (b), (e), and (h), it can be seen that a higher C_{flex} and a larger BES lead to larger p^{flex} in Case A. In Case B, however, the shorter notice limited p^{flex} from the smaller BES, which did not exceed the amount of 34.7 kW despite the increase in C_{flex}. Nevertheless, this BES could offer more flexibility than the 14.4 kWh BES (and even the 18 kWh BES at very low C_{flex}) for reasons explained in Section V-B1 i.e., higher need to increase value through the FS due to lower potential for energy and peak power cost reduction (or profit from energy arbitrage). Fig. 7 (h) shows the average flexibility bids and their range for the 7.2 kWh BES. The results from other BESs are omitted for clarity purposes, however, they exhibit the same trend, such that the BES size and C_{flex} do not affect the average p^{flex} in Case C.

3) Effect of Degradation: Although with the tested flexibility prices the value of flexibility dispatch remained practically unaffected by the BES size as can be seen in Fig. 7 (a), (d), and (g), the faster degradation of smaller BESs suggests that the investment on the size of a BES that will provide FSs should be determined considering the frequency of providing these FSs. Fig. 7 (c), (f), (i) depict the degradation cost as a percentage of the BES's purchase cost, where both cycle and calendar aging were considered. Calendar aging was assessed after the simulations, as it was not included in the objective function (see [20]), which explains why e.g., in Fig. 7 (c), there is a significant decrease in the degradation cost of the 7.2 kWh BES when C_{flex} increases. Comparing the different BES sizes it can clearly be seen that the induced aging is worse for the smallest BES. This is more notable in Fig. 7 (c) and (f) and it can be attributed to the increased utilization (cycling) in an attempt to maximize profit from both ESs and FSs. If the FS is event-based (e.g., requested during extreme weather conditions or unexpected failures) the effect of degradation would be trivial. Otherwise, long-term planning studies are required to assess whether the faster degradation of smaller BESs could result in a reduced value of their flexibility.

An example of the different BES utilization is shown in Fig. 8, which depicts the MG power flows for Case A, C_{flex} = 0.4\$/kW and E^{max} = 14.4 kWh, comparing the results with and without the FS. Without the FS, the BES was only discharged after the flexibility period, when peak demand was expected (time steps 86-90). When the MG offered flexibility (Fig. 8 (a)), the BES's utilization increased, as it started charging at $\tau = t_0$ to be able to inject power both at time steps 86-90 and within the activation period.

D. Number of Scenarios and Cost of Optimal Solution

Since all the studied SO problems were linear, the convergence to an optimal solution is guaranteed at each time step. However, the optimality with respect to all possible uncertainty realizations cannot be guaranteed. Scenario-based approaches are based on samples and, therefore, there is a trade-off between the cost of the solution and the execution time. A higher number of scenarios can lead to a lower cost i.e., a solution closer to the optimal solution, however, it also increases the computation time. To investigate the relationship between scenario number, optimality and computation time, a sensitivity analysis was performed for Case A, with E^{max} =7.2 kWh and C_{flex} = 0.4 \$/kW. The results are given in Table III, where the performance of the case study implemented in this work is shown in bold and the negative cost value refers to profit. Since the sampling happens at two

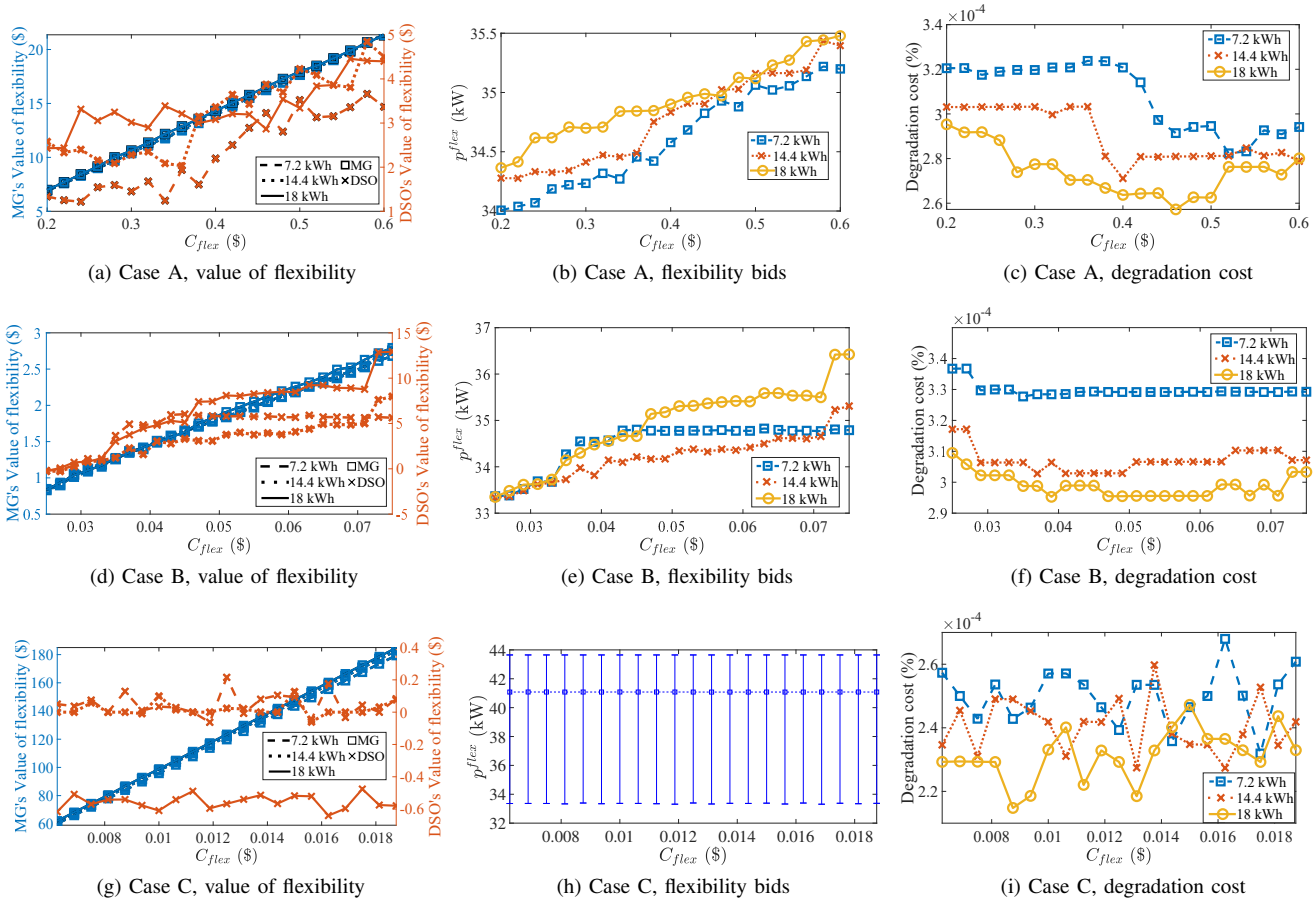

(a) Case A, value of flexibility (b) Case A, flexibility bids (c) Case A, degradation cost

(d) Case B, value of flexibility (e) Case B, flexibility bids (f) Case B, degradation cost

(g) Case C, value of flexibility (h) Case C, flexibility bids (i) Case C, degradation cost

Fig. 7: The flexibility bid, value of flexibility, and BES degradation cost w.r.t. C_{flex} for Cases A-C.

stages in this paper i.e., first with the MC method and then with the scenario reduction, the analysis accounted for both sample sizes. The execution time refers to the maximum time that was needed for scenario generation, scenario reduction (if applicable), and for the solution of the SO problem.

It can be observed from Table III that scenario reduction, when considered, accounts for the biggest part in total execution time. For example, a SO problem with 80 scenarios is solved in 9, 34, and 59 sec when obtained from a full set of 2000, 4000, and 5000 scenarios, respectively. Nevertheless, the scenario reduction leads to a significant decrease in execution time, as it reduces the number of variables of the SO problem. The daily cost, which is shown in the last column of Table III, was not directly comparable for the studied sizes of scenario sets, even when no scenario reduction was implemented. This occurs due to the random scenario generation and the RH, since 96 solutions of the SO problem are needed to obtain the daily cost. Despite that, the cost did not vary significantly, and the results yielded a maximum variation of 1.7% from the average cost obtained by these scenario sets.

The results demonstrated that the number of scenarios used in the case study was sufficient for the study's MG, as the cost did not deviate considerably among the scenario sets of the sensitivity analysis. Although there was no proven economic benefit, the larger sets of Table III could also be used, since their respective solution time was compatible with the chosen time step. Larger sets might not be preferable for real-world applications, however, as communication delays associated with input and output data must also be accounted for.

TABLE III: Scenario Sensitivity Analysis for Case A, E^{max} =7.2 kWh, $C_{flex} = 0.4$ \$/kW.

Full set	Reduction	Reduced set	Execution time (sec)	Cost ($)
5000	no	–	111	-3.58
5000	yes	120	75	-3.66
5000	yes	80	59	-3.69
4000	no	–	81	-3.57
4000	yes	120	45	-3.66
4000	yes	80	34	-3.69
2000	no	–	24	-3.58
2000	**yes**	**120**	**11**	**-3.68**
2000	yes	80	9	-3.69

VI. Conclusions

This paper presents a scenario-based SO model to solve the MG energy and flexibility dispatch problem considering uncertainties in PV generation and electric load demand. A

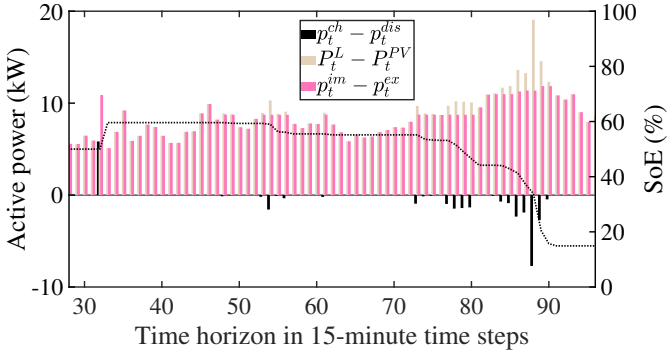

(a) With FS

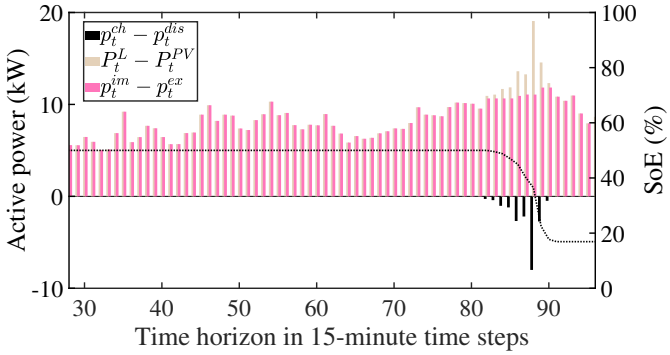

(b) Without FS

Fig. 8: MG power flows with and without FS for Case A with $C_{flex} = 0.4\$/kW$ and $E^{max} = 14.4$ kWh.

detailed model of a FS known as capacity limitation was also incorporated in the proposed model. The SO model was combined with the RH approach, which ensured the dispatch of flexibility according to the bid in all simulations for Cases A-C. Thus, the payment of penalties was avoided, which increased the economic value of flexibility for the MG. This value was at least 56% and 7% of the daily MG operation cost under the considered C_{flex} in Cases A-B, respectively. These cases, unlike Case C, also benefited the DSO suggesting that DSOs might have little to gain from high-resolution flexibility dispatch for the purpose of reducing the daily peak. Increasing the BES size did not significantly affect the daily value of MG's flexibility, however, long-term studies could give different results, as the degradation cost was found to be smaller with the larger BESs. The simulations also showed that the 7.2 kWh BES could provide more flexibility than the 14.4 kWh BES depending on the notification time and C_{flex}, as the MG would benefit more from using the additional capacity of the larger BES for ESs instead of the FS.

The methodology for flexibility assessment and dispatch, which was introduced to test the performance of the developed model, is versatile and can be applied to a wide range of case studies e.g., with different notification times or periods of flexibility activation. This model can be used by the MG operators to quantify the potential and assess the value of MG flexibility. The same model with minor modifications can also be used to derive the bidding curve of the MG in case the DSO operates a local flexibility market to procure flexibility, which is a suggestion for future studies. Aside from the MG operators, the grid operators can also benefit from the methodology of flexibility assessment, which can contribute to formulating the flexibility prices or incentives that would lead to the dispatch of the desired flexibility depending on the system's needs. In addition, the computational efficiency of the proposed approach confirms that flexibility can be dispatched promptly (close to real-time) within a day, which could contribute to the reduction of grid capacity reserves if multiple MGs participate in the provision of the FS.

REFERENCES

[1] F. Garcia-Torres *et al.*, "Cooperative optimization of networked microgrids for supporting grid flexibility services using model predictive control," *IEEE Trans. Smart Grid*, vol. 12, no. 3, pp. 1893–1903, 2021.

[2] A. Shakoor *et al.*, "Roadmap for flexibility services to 2030," *A report to the Committee on Climate Change. London: Pöyry*, 2017.

[3] S. Repo *et al.*, "The ide4l project: defining, designing, and demonstrating the ideal grid for all," *IEEE Power and Energy Mag.*, vol. 15, no. 3, pp. 41–51, May-June 2017.

[4] S. Klyapovskiy *et al.*, "Utilizing flexibility services from a large heat pump to postpone grid reinforcement," in *Proc. IEEE Student Conf. Elect. Machines and Syst.*, Huzhou, China, 14-16 Dec. 2018.

[5] G. Tian, Q. Z. Sun, and W. Wang, "Real-time flexibility quantification of a building hvac system for peak demand reduction," *IEEE Trans. Power Syst.*, to be published.

[6] Y. Huo *et al.*, "Decision tree-based optimization for flexibility management for sustainable energy microgrids," *Applied Energy*, vol. 290, p. 116772, May 2021.

[7] R. Vincent *et al.*, "Residential microgrid energy management considering flexibility services opportunities and forecast uncertainties," *Int. J. Elect. Power & Energy Syst.*, vol. 120, p. 105981, Sep. 2020.

[8] P. MacDougall *et al.*, "Applying machine learning techniques for forecasting flexibility of virtual power plants," in *Proc. IEEE Elect. Power and Energy Conf. (EPEC)*, Ottawa, ON, Canada, 12-14 Oct. 2016.

[9] W. Alharbi and K. Bhattacharya, "Incentive design for flexibility provisions from residential energy hubs in smart grid," *IEEE Trans. Smart Grid*, vol. 12, no. 3, pp. 2113–2124, May 2021.

[10] M. MansourLakouraj *et al.*, "Exploitation of microgrid flexibility in distribution system hosting prosumers," *IEEE Trans. Ind. Applications*, vol. 57, no. 4, pp. 4222–4231, July/Aug. 2021.

[11] ——, "Optimal power management of dependent microgrid considering distribution market and unused power capacity," *Energy*, p. 117551, June 2020.

[12] C. Ziras *et al.*, "Why baselines are not suited for local flexibility markets," *Renewable and Sustainable Energy Reviews*, vol. 135, p. 110357, Jan., 2021.

[13] N. Nazir and M. Almassalkhi, "Grid-aware aggregation and realtime disaggregation of distributed energy resources in radial networks," *IEEE Trans. Power Systems*, to be published.

[14] Y. Song *et al.*, "Aggregated power flexibility of active distribution network considering reliability and uncertainty," in *Proc. IEEE/IAS Ind. and Commercial Power Syst. Asia (ICPS Asia)*, Weihai, China, 13-15 July 2020.

[15] D. Lee *et al.*, "Robust ac optimal power flow with robust convex restriction," *IEEE Trans.Power Systems*, vol. 36, no. 6, pp. 4953–4966, Apr. 2021.

[16] J. Villar *et al.*, "Flexibility products and markets: Literature review," *Electric Power Syst. Research*, vol. 154, pp. 329–340, Jan. 2018.

[17] C. Ziras *et al.*, "A mid-term DSO market for capacity limits: How to estimate opportunity costs of aggregators?" *IEEE Trans. Smart Grid*, vol. 11, no. 1, pp. 334–345, Jan. 2020.

[18] K. Abdulla *et al.*, "Optimal operation of energy storage systems considering forecasts and battery degradation," *IEEE Trans. Smart Grid*, vol. 9, no. 3, pp. 2086–2096, May 2018.

[19] A. J. Gonzalez-Castellanos *et al.*, "Non-ideal linear operation model for Li-ion batteries," *IEEE Trans. Power Syst.*, vol. 35, no. 1, pp. 672–682, Jan. 2020.

[20] K. Antoniadou-Plytaria *et al.*, "Market-based energy management model of a building microgrid considering battery degradation," *IEEE Trans. Smart Grid*, vol. 12, no. 2, pp. 1794–1804, Mar. 2021.

[21] J. Wang *et al.*, "Degradation of lithium ion batteries employing graphite negatives and nickel–cobalt–manganese oxide+ spinel manganese oxide positives: Part 1, aging mechanisms and life estimation," *J. of Power Sources*, vol. 269, pp. 937–948, Dec. 2014.
[22] D. Wang *et al.*, "Quantifying electric vehicle battery degradation from driving vs. vehicle-to-grid services," *J. of Power Sources*, vol. 332, pp. 193–203, Nov. 2016.
[23] G. Cardoso *et al.*, "Battery aging in multi-energy microgrid design using mixed integer linear programming," *Applied Energy*, vol. 231, pp. 1059–1069, Dec. 2018.
[24] H. Kim *et al.*, "Direct energy trading of microgrids in distribution energy market," *IEEE Trans. Power Syst.*, vol. 35, no. 1, pp. 639–651, July 2019.
[25] A. Perez *et al.*, "Effect of battery degradation on multi-service portfolios of energy storage," *IEEE Trans. Sust. Energy*, vol. 7, no. 4, pp. 1718–1729, Oct. 2016.
[26] W. B. Powell and S. Meisel, "Tutorial on stochastic optimization in energy—part i: Modeling and policies," *IEEE Trans. Power Syst.*, vol. 31, no. 2, pp. 1459–1467, Apr. 2015.
[27] Y. Zhang *et al.*, "A stochastic MPC based approach to integrated energy management in microgrids," *Sustainable Cities and Soc.*, vol. 41, pp. 349–362, Aug. 2018.
[28] W. B. Powell, "A unified framework for stochastic optimization," *Eur. J. Oper.Res.*, vol. 275, no. 3, pp. 795–821, June 2019.
[29] A. Ben-Tal and A. Nemirovski, "Robust convex optimization," *Mathematics of Operations Research*, vol. 23, no. 4, pp. 769–805, Nov. 1998.
[30] J. S. Giraldo *et al.*, "Microgrids energy management using robust convex programming," *IEEE Trans. Smart Grid*, vol. 10, no. 4, pp. 4520–4530, July 2019.
[31] K. Margellos *et al.*, "On the road between robust optimization and the scenario approach for chance constrained optimization problems," *IEEE Trans. Automat. Control*, vol. 59, no. 8, pp. 2258–2263, Aug. 2014.
[32] E. Mocanu *et al.*, "On-line building energy optimization using deep reinforcement learning," *IEEE Trans. Smart Grid*, vol. 10, no. 4, pp. 3698–3708, May 2018.
[33] H. Shuai *et al.*, "Optimal real-time operation strategy for microgrid: An ADP-based stochastic nonlinear optimization approach," *IEEE Trans. Sust. Energy*, vol. 10, no. 2, pp. 931–942, Apr. 2019.
[34] A. Ehsan and Q. Yang, "Scenario-based investment planning of isolated multi-energy microgrids considering electricity, heating and cooling demand," *Applied Energy*, vol. 235, pp. 1277–1288, Feb. 2019.
[35] B. V. Solanki *et al.*, "Including smart loads for optimal demand response in integrated energy management systems for isolated microgrids," *IEEE Trans. Smart Grid*, vol. 8, no. 4, pp. 1739–1748, July 2017.
[36] Nord Pool. [Online]. Available: https://www.nordpoolgroup.com/
[37] HSB, "HSB living lab." [Online]. Available: https://www.hsb.se/hsblivinglab/
[38] Göteborg Energi. [Online]. Available: https://www.goteborgenergi.se/
[39] B. V. Mbuwir *et al.*, "Reinforcement learning for control of flexibility providers in a residential microgrid," *IET Smart Grid*, vol. 3, no. 1, pp. 98–107, Feb. 2020.
[40] E.ON. E.ON' swtich flexibility market. [Online]. Available: https://www.eon.se/foeretag/elnaet/switch/marknader-produkter

Kyriaki Antoniadou-Plytaria (Graduate Student Member, IEEE) received the diploma in Electrical and Computer Engineering from the National Technical University of Athens (NTUA), Greece, in 2016. Currently, she is pursuing the Ph.D. degree at Chalmers University of Technology, Gothenburg, Sweden. Her research interests are the modeling and optimization of the smart grid and microgrid operation considering integration of distributed energy resources.

David Steen received the M.Sc. and Ph. D. degrees in electrical engineering from the Chalmers University of Technology in 2008 and 2014, respectively. Currently, he is a researcher in the Department of Electrical engineering, Chalmers University of Technology, Gothenburg, Sweden. His research interests include modeling and control of integrated energy systems and distributed energy resources such as solar PV, wind power, electric vehicles, energy storages.

Le Anh Tuan (S'01, M'09) received the BSc degree in power systems from Hanoi University of Technology, Vietnam in 1995, the MSc degree in energy economics from the Asian Institute of Technology, Thailand in 1997, and the PhD degree in power systems from the Chalmers University of Technology, Sweden in 2004. He is currently an Associate Professor at the Division of Electric Power Engineering, Department of Electrical Engineering, Chalmers University of Technology. His current research interests include: Modelling, optimization, control and protection of integrated energy systems and intelligent distribution networks with high level of renewables and energy storages; Wide-area monitoring and control of power transmission systems; Machine learning applications to power systems; Modelling, design and analysis of energy and ancillary service markets.

Ola Carlson was born in Onsala, Sweden 1955. He received the M.Sc. and Ph.D. degree in Electrical Engineering from Chalmers University of Technology, Gothenburg, Sweden in 1980 and 1988, respectively. He is currently a Professor at the Department of Electrical Engineering at Chalmers University of Technology. His major interests are electrical systems for renewable power production, especially wind power, smart grid and hybrid electric vehicles.

Baraa Mohandes (M'09) received his BSc. (2010) degree in Electrical Engineering from Khalifa University, the Petroleum Institute, UAE, where he was the recipient of the Abu-Dhabi National Oil Company's (ADNOC) scholarship. Following his BSc., he worked as a technical support and projects engineer in one of ADNOC's subsidiaries in the oil&gas industry from (2010) to (2015). He also completed his MSc. degree in 2015 from Khalifa University. In 2016, he was awarded the Masdar Institute's (MI) fellowship for the joint MI and Massachusetts Institute of Technology Program for the PhD in Interdisciplinary Engineering, and received his PhD degree in 2020 for his work on power systems optimization and economics. Following the completion of his PhD, he joined the Luxembourg Institute of Science in Technology (LIST) as a postdoctoral research associate. His research interests are diverse, and include feedback control systems, and power system applications of data science, optimization, complex networks theory, and game-theory.

Mohammad Ali Fotouhi Ghazvini received the M.Sc. degree in electrical engineering from the K. N. Toosi University of Technology, Iran, in 2009, and the Ph.D. degree in electrical engineering from the University of Lisbon, Portugal, in 2018. He was a Researcher with the Department of Electrical Engineering, Chalmers University of Technology, Gothenburg, Sweden. His research interests include the operation and control of integrated multi-energy systems, energy management systems, and power system analysis and scheduling.